Ionics
DOI 10.1007/s11581-017-2273-9

ORIGINAL PAPER

# Preparation and characterization of blend polymer electrolyte film based on poly(vinyl alcohol)-poly(acrylonitrile)/$MgCl_2$ for energy storage devices

**R. Manjuladevi [1,2] · M. Thamilselvan [3] · S. Selvasekarapandian [2,4] · P. Christopher Selvin [4] · R. Mangalam [5] · S. Monisha [2,6]**

Received: 31 July 2017 / Revised: 27 August 2017 / Accepted: 5 September 2017


**Abstract** The development of magnesium electrolytes for battery applications has been the demand for electrochemical devices. To meet such demand, in this work solid blend polymer electrolytes were prepared using polyvinyl alcohol (PVA) and polyacrylonitrile (PAN) (92.5PVA:7.5PAN) as host polymer, magnesium chloride ($MgCl_2$) of different molar mass percentage (m.m.%) (0.1, 0.2, 0.3, 0.4, 0.5, and 0.6%) as salt and dimethylformamide (DMF) as solvent. Structural, vibrational, thermal, electrical, and electrochemical properties of the prepared electrolytes were investigated using different techniques such as X-ray diffraction pattern, FTIR spectroscopy analysis, differential scanning calorimetry (DSC), AC impedance measurement, and transference number measurement. X-ray diffraction studies confirm the minimum volume fraction of crystalline phase for the polymer electrolyte with 0.5 m.m.% of $MgCl_2$. FTIR confirms the complex formation between host polymer and salt. DSC analysis proves the thermal transition of the prepared films are affected by salt concentration. The optimized material with 0.5 m.m.% of $MgCl_2$ offers a maximum electrical conductivity of $1.01 \times 10^{-3}$ S $cm^{-1}$ at room temperature. The $Mg^{2+}$ ion conduction in the blend polymer electrolyte is confirmed from transference number measurement. Electrochemical analysis demonstrates the promising characteristic of these polymer films suitable as electrolytes for primary magnesium batteries. Output potential and discharge characteristics have been analyzed for primary magnesium battery which is constructed using optimized conducting electrolyte.

**Keywords** Blend polymer electrolyte · Polyacrylonitrile · Magnesium chloride · Ionic conductivity · Primary magnesium battery

✉ S. Selvasekarapandian
sekarapandian@rediffmail.com

[1] Department of Physics, SNS College of Engineering, Coimbatore, Tamil Nadu, India

[2] Materials Research Center, Coimbatore, Tamil Nadu, India

[3] Department of Physics, Thanthai Periyar Government Institute of Technology, Vellore, Tamil Nadu, India

[4] Department of Physics, Bharathiar University, Coimbatore, Tamil Nadu, India

[5] Department of Physics, PSG Institute of Technology and Applied Research, Coimbatore, Tamil Nadu, India

[6] Department of Physics, N.M.S.S. Vellaichamy Nadar College, Madurai, Tamil Nadu, India

## Introduction

Solid polymer electrolyte (SPE) systems have attracted prevalent attention for the fabrication of all solid state electrochemical devices. Among them for metal-ion rechargeable batteries, SPE's are attractive due to their promising advantages, including safety, ease of packing, excellent flexibility, and low level of environmental pollution [1, 2]. For the development of SPE's, various polymers have been employed such as PEO [3], PPO [4], PVA [5], PVC [6], PVDF [7], and PMMA [8]. Researches have been done on polymer/polymer blends in order to improve electrochemical stability, conductivity, chemical and electrochemical compatibility with electrode materials with good thermal and dimensional stability [9] and it has been shown that polymer electrolytes based on blends possess higher conductivity compared to polymer electrolytes based on individual host polymer. The conductivity of PVdf-co-HFP polymer complex when blended with PEMA has been found to be in the order of $10^{-3}$ S $cm^{-1}$ [10]. A PVA/PMMA blend polymer electrolyte (BPE) was reported

Published online: 18 September 2017

to have an improved conductivity of $1.28 \times 10^{-3}$ S cm$^{-1}$ when compared to pure PVA ($2 \times 10^{-10}$ S cm$^{-1}$) [11]. Further many blend electrolytes have been reported to achieve better conductivity based on PVP/PVA [12], PVA/PAN [13], PVDF-HFP/PEMA [14], and so on.

Among the polymers reported, poly(vinyl alcohol) (PVA) is a semi-crystalline, highly abundant, non-toxic, and biocompatible polymer with good chemical and thermal stability. It contains hydroxyl groups attached to methane carbons which acts as carbon chain backbone. These OH groups which can be a source of hydrogen bonding assist in the formation of polymer blends [15, 16]. Polyacrylonitrile (PAN) polymer has been extensively studied due to their good chemical, flame resistance, and electrochemical stability [17]. Polyacrylonitrile (PAN) is a semicrystalline, synthetic resin which is one of the most important fiber-forming polymers and has been widely used because of its high strength and abrasion resistance [18]. Both of the polymers PVA and PAN are soluble in dimethylformamide (DMF).

Due to their high-energy density values, Li-ion battery technology has been widely employed in energy supply and storage systems. However, the high cost, decrease of abundance, environmental impact and safety limitations concerning to lithium materials impede their widespread implementation in future battery technologies [19]. Therefore, it is necessary to search for alternative energy storage system technology capable of complementing the Li-ion battery technology. Among the accessible battery chemistries, magnesium-based batteries have recently captured much attention because they are environmentally friendly, non-toxic, low cost, and earth abundant material. Magnesium metal possesses a number of characteristics which make it attractive as a negative electrode material for rechargeable batteries; high negative standard potential (− 2.375 V versus SHE), relatively low equivalent weight (12 g per Faraday), high melting point (649 °C), low cost, relative abundance, high safety, ease of handling, and low toxicity which allows for urban waste disposal. In resemblance to the rechargeable lithium battery system, the solid state rechargeable magnesium battery requires a $Mg^{2+}$ ion conducting polymer electrolyte. Mangalam et al. reported that the incorporation of $Mg(ClO_4)_2$ enhances the ionic conductivity of blend PVA/PVP to $1.1 \times 10^{-4}$ S/cm at RT [20]. Selladurai et al. has reported that $MgCl_2$ could coordinate with PEO and the ionic conductivity increases with increasing in salt content [21]. Pandey et al. studied the interaction of $Mg(CF_3SO_3)_2$ and PVdF-HFP and found that ionic conductivity increased with salt content [22].

The present work is aimed at synthesizing a blend polymer electrolyte with PVA and PAN having high conductance property. The ionic conductivity of pure PVA ($2 \times 10^{-10}$ Scm$^{-1}$) increases to $1.13 \times 10^{-7}$ S cm$^{-1}$ at room temperature for the composition 92.5PVA:7.5PAN [18]. A few researchers have reported studies on lithium and ammonium ion conducting polymer electrolytes employing this 92.5PVA:7.5PAN polymer blend as host [23–26]. However, magnesium conducting polymer electrolytes based on this blend are scanty in literature. The rate of electrochemical deposition of host polymer was found to increase as a function of the nature of chloride anions present [27]. In this paper, we report the effect of magnesium chloride ($MgCl_2$) on BPE 92.5PVA:7.5PAN in improving its conductivity. The BPE 92.5PVA:7.5PAN with $MgCl_2$ of different concentrations have been prepared using solution casting technique and have been characterized by X-ray diffraction (XRD), Fourier transform infrared spectroscopy (FTIR), differential scanning calorimetry (DSC), electrochemical impedance spectroscopic analysis, and battery discharge studies.

## Experimental technique

Polyvinyl alcohol (PVA) with an average molecular weight of 1,25,000 from Sd fine-chem Ltd., polyacrylonitrile (PAN) with an average molecular weight of 1,50,000 from Sigma Aldrich and magnesium perchlorate ($Mg(ClO_4)_2$) of molecular weight 223.21 g/mol from Himedia were used without any further purification to prepare the blend polymer electrolytes. Dimethylformamide (DMF) with molecular weight 73.08 g/mol, density = 0.948–0.949 kg/m$^3$ from Merck specialties private Ltd., has been used as solvent.

Blended polymer electrolyte (BPE) films 92.5PVA:7.5PAN and $MgCl_2$ complex have been prepared by solution cast-technique with different concentrations. Initially 92.5 wt% of PVA was added to the solvent DMF at 50 °C and stirred continuously until the complete dissolution of the polymer in the solvent. Then 7.5 wt% of PAN is added to the solution and stirred continuously to get a clear solution. Then a required quantity of $MgCl_2$ of various m.m.% (0.05, 0.1, 0.15, 0.2, 0.25, and 0.3%) was added and the resultant solution was stirred continuously until a clear homogeneous solution is obtained.

Then the solution has been transferred into petri dish and dried at 60 °C for 2 days to eliminate the solvent. After drying, the transparent flexible films of thickness ranging from 150 to 200 μm were obtained. The obtained films were taken for further characterization.

### Characterization techniques

#### *X-ray diffraction (XRD) analysis*

The amorphousity of BPE has been investigated using XRD. The XRD patterns of the films were recorded at room temperature by X' pert pro diffractometer system using the Cu-K$\alpha$ radiation in the range of $2\theta$ = 10°–90°.

*Vibrational analysis*

The complex formation between the chemical constituents in the PVA:PAN polymer matrix and $MgCl_2$ has been analyzed by using FTIR. ALPHA BRUKER FT-IR spectrophotometer has been used to record the FTIR spectrum in the wavenumber range 3000–500 $cm^{-1}$ at room temperature.

*Thermal analysis*

The thermal behavior of the prepared samples were studied using a differential scanning calorimeter (DSC) (Perkin Elmer DSC 4000 apparatus). The samples were heated from 20° to 200 °C in $N_2$ atmosphere at a heating rate of 20 °C/min.

*Electrochemical impedance spectroscopy (EIS) analysis*

For characterizing the ionic conductivity of the electrolyte film, impedance analysis has been performed using impedance spectrometer. The impedance of the prepared polymer electrolytes were recorded using computer controlled HIOKI 3532-50 LCR Hi-Tester in the frequency range between 42 Hz and 1 MHz with the temperature range of 303–353 K using stainless steel (SS) as the blocking electrodes.

*Transference number measurement (TNM)*

The total ionic transport number ($t_{ion}$) was obtained by the d.c. polarization technique [28]. In this technique, a SS|92.5PVA:7.5PAN:0.5 m.m.% $MgCl_2$|SS cell was polarized by applying a step potential of 1.5 V and the resulting potentiostatic current was monitored as a function of time. Stainless steel (SS) acted as blocking electrodes for the above cell. The '$t_{ion}$' was evaluated using the formula:

$$t_{\text{ion}} = \frac{i_T - i_e}{i_T} \quad (1)$$

where $i_T$ and $i_e$ are total and residual current, respectively. The $Mg^{2+}$ ions transport number ($t^+$) of BPE was evaluated using a combination of AC impedance spectroscopy and DC polarization studies on a Mg|BPE|Mg cell according to the method of Evans et al. [29].

*Electrochemical stability analysis*

Electrochemical stability is an important criterion to investigate the working cell potential of an electrolyte. Using linear sweep voltammetry, the working potential of the BPE has been measured by stainless steel as the working electrode and Mg disc as combined counter and the reference electrodes.

*Preparation of anode, cathode, and fabrication of proton battery*

The primary magnesium battery was constructed by using the highest conductivity BPE membrane. The desired composition of manganese dioxide and graphite powder in the ratio 3:1 were mixed together and grounded well using mortar. Few drops of the polymer electrolyte was added to reduce the electrode polarization [30] and the final mixture was pelletized to form the cathode (thickness = 1.9 mm). Magnesium metal of thickness 1 mm and dia 0.6 mm was used as anode. The battery was constructed using the above mentioned anode and cathode with the maximum conducting polymer electrolyte. The overall battery thickness was found to be 5.5 mm. The performance of the battery was studied.

## Result and discussion

### X-ray diffraction analysis (XRD)

Figure 1 represents XRD patterns of pure BPE (92.5PVA:7.5PAN) and its complexes with $MgCl_2$ salt at different concentrations (0.4 m.m.%, 0.5 m.m.%, 0.6 m.m%.). It is evident from the XRD measurements that the 92.5PVA:7.5PAN BPE displays intense diffraction peaks at $2\theta$ = 20.3° and 40.8° corresponding to characteristic crystalline peak of pure PVA [24]. The gradual decrease in intensity and increase of broadness of the diffraction peaks as a function of complexation of $MgCl_2$ salt (Fig. 1b–d) reveal the decrease in crystallinity of BPE due to the interaction of the salt with the polymer. The crystallite size for all the electrolytes have been calculated using Debye-Scherer's equation [31]

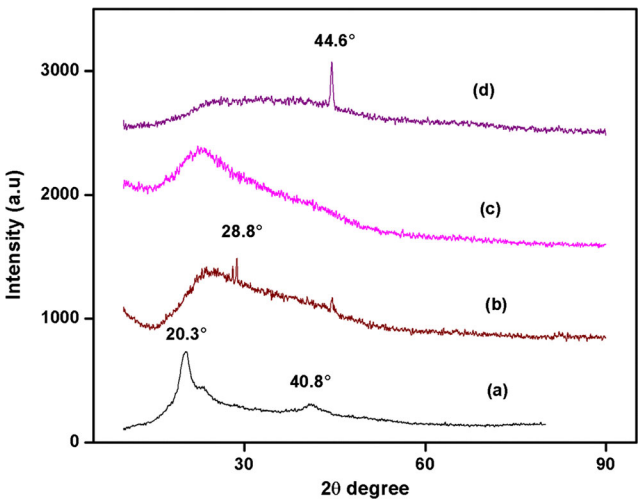


**Fig. 1** XRD patterns of BPE's (a) 92.5PVA:7.5PAN, (b) 92.5PVA:7.5PAN: 0.4 m.m.% $Mg(Cl)_2$, (c) 92.5PVA:7.5PAN:0.5 m.m.% $Mg(Cl)_2$, and (d) 92.5PVA:7.5PAN:0.6 m.m.% $Mg(Cl)_2$

**Table 1** Diffraction peak, crystallite size, and relative intensity of BPE's

| Composition | Diffraction peak (2θ) | Crystallite size (nm) | Relative intensity % |
|---|---|---|---|
| 92.5PVA:7.5PAN | 20.47 | 5.48 | 100 |
| 92.5PVA:7.5PAN:0.4 m.m. % MgCl2 | 24.38 | 3.08 | 62.4 |
| 92.5PVA:7.5PAN:0.5 m.m. % MgCl2 | 23.14 | 2.19 | 44.6 |
| 92.5PVA:7.5PAN:0.6 m.m. % MgCl2 | 24.2 | 4.21 | 57.8 |

$$D = \frac{0.89\,\lambda}{\beta cos\,\theta} \quad (2)$$

where $\lambda$ is the wavelength of the X-ray source, $\beta$ is the fullwidth of the half maximum (FWHM), and $\theta$ is the diffraction angle. The diffraction angle, crystallite size, and relative intensities of all electrolytes have been tabulated in Table 1. It is observed that 92.5PVA:7.5PAN:0.5 m.m.% $MgCl_2$ polymer electrolyte has got small crystallite size and less relative intensity. The decrease of the relative intensity with increase in fullwidth half maximum of the characteristic peak reveals the amorphous nature of the polymer electrolyte. These results can be interpreted in terms of the Hodge et al. criterion which has established a correlation between the height of the peak and the degree of crystallinity [32]. The high amorphous nature is found at 0.5 m.m.% salt to host polymer when compared with other polymer electrolyte samples. The increase in the amorphous nature causes a reduction in the energy barrier to the segmental motion of the polymer electrolyte resulting in high ionic conductivity [33]. In the present case, however, peak shifting and emergence of new peaks is observed. The peaks at $2\theta = 14.9°, 28.2°, 30.1°, 32.1°, 41.7°, 45.8°, 50°$, and 52.5° are observed for pure magnesium chloride (JCPDS card number: 72-1517). Among them, the peaks at 28° and 44° with less intense have been observed for the composition 0.4 m.m% of $MgCl_2$. Peak at 44° has been absorbed for 0.6 m.m% of $MgCl_2$. These peaks correspond to the recrystallization of added salt. With increasing salt content, $Mg^{2+}$ ion swells the crystalline of the host polymer [34]. Hence, the X-ray diffraction analysis reveals amorphous nature in the polymer matrices.

## Fourier transform infrared (FTIR) spectroscopy analysis

The FTIR spectra of pure PVA, PAN and host blend polymer 92.5PVA:7.5PAN recorded at room temperature in the region 500–4000 $cm^{-1}$ is shown in Fig. 2A. From Fig. 2A, the band at about 3305 $cm^{-1}$ assigned to OH stretching of pure PVA [35] is moved to 3293 $cm^{-1}$ for the BPE 92.5PVA:7.5PAN. The bands corresponding to methylene group ($CH_2$) asymmetric stretching and C=O stretching vibrations of pure PVA occurs at 2925 and 1732 $cm^{-1}$ [36] which have been shifted to 2926 and 1723 $cm^{-1}$ respectively in host blend polymer 92.5PVA:7.5PAN. The bands at 1379, 1244, and 1094 $cm^{-1}$ have been assigned to $CH_3$ symmetric, C-O-C stretching, and C-O stretching of acetyl group present on the PVA backbone [37, 38]. These bands get shifted to 1377, 1246, and 1095 $cm^{-1}$ in 92.5PVA:7.5PAN. The vibrational peak at 2244 $cm^{-1}$ for pure PAN represents the stretching vibration of C≡N stretching [39, 40] which is the most characteristic band of PAN has been shifted to 2236 $cm^{-1}$ in pure blend 92.5PVA:7.5PAN. The vibrational bands at 2944, 1666, and 1254 $cm^{-1}$ which have been assigned to $CH_2$ stretching vibration, C=C stretching vibration, and CH wagging in pure PAN

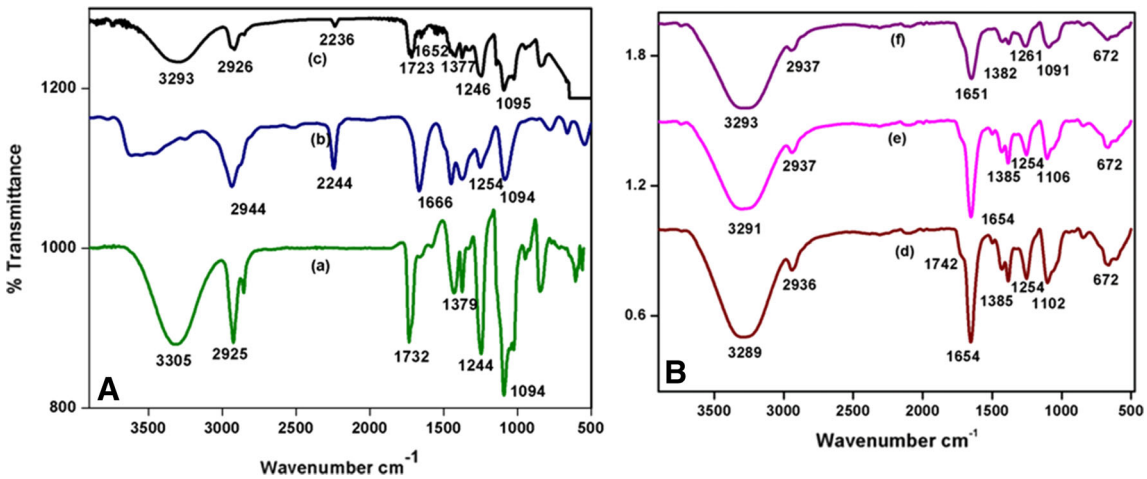


**Fig. 2** **A**- FTIR spectra for (a) pure PVA, (b) pure PAN, and (c) 92.5PVA:7.5PAN polymer electrolyte. **B**- With different $MgCl_2$ concentrations (d) 0.4 m.m. %, (e) 0.5 m.m%, and (f) 0.6 m.m. %

have been absent in the host blend polymer which indicates the complex formation during blending.

Figure 2B shows the FTIR spectra of pure 92.5PVA:7.5PAN and 92.5PVA:7.5PAN added with three different concentrations (0.4 m.m.%, 0.5 m.m.%, and 0.6 m.m.%) of $MgCl_2$ and the corresponding vibrational frequencies were assigned and listed in Table 2. A broad peak centered around 3293 $cm^{-1}$ in 92.5PVA:7.5PAN assigned to the stretching vibration of hydroxyl group of pure PVA gets shifted and broadened when the salt $MgCl_2$ of different concentrations (0.4 m.m.%, 0.5 m.m.%, and 0.6 m.m.%) are added. This indicates the coordination between the cation of the salt and hydroxyl group of PVA [41]. $Mg^{2+}$ and $Cl^{2-}$ were an electrophile which seeks electron rich atom and nucleophile which seeks electron deficient atom respectively to make possible interaction with hydroxyl oxygen and hydroxyl hydrogen of the polymer chain resulting in the decrease in intensity and broadening of the O–H peak in the polymer complexes [42]. In consistent with the XRD results, the crystallinity of the PVA is altered due to the interaction of the cation/anion of the salt with the O-H group of PVA. The detected peaks for pure 92.5PVA:7.5PAN are $CH_2$ asymmetric stretching, C = C stretching, $CH_3$ symmetric, C-O-C stretching, and C-C asymmetric at bands 2926, 1652, 1377, 1246, and 1095 $cm^{-1}$, respectively, get shifted with decrease in intensity of the bands when the salt concentration is introduced.

Figure 3 shows the possible interaction between the host polymer with the salt. The carbonyl group (C = O) stretching vibration shifts due to the addition of salt which implies that strong intermolecular interaction is between magnesium ion present in salt and oxygen atoms resulting in polymer salt complexes. The coordinate bond with magnesium ion is formed by the oxygen atoms from PVA, which is expected to act as electron donor atoms [43]. The shift in stretching modes of the carbonyl bonds has been seen for the sample with 0.4 m.m.% of salt and disappearance of the peak is seen for rest of the electrolytes which indicates complexation of the polymer. Due to the addition of $MgCl_2$ from 0.4 to 0.6 m.m.%,

**Table 2** FTIR assignments of the calculated and observed vibrational frequencies of 92.5PVA:7.5PAN: $MgCl_2$ BPE's

| 92.5PVA:7.5PAN: x m.m.% | | | | Assignments |
|---|---|---|---|---|
| 0 | 0.4 | 0.5 | 0.6 | |
| 3293 | 3289 | 3291 | 3293 | OH stretching |
| 2926 | 2936 | 2937 | 2937 | $CH_2$ asymmetric stretching |
| 2236 | – | – | – | C ≡ N stretching vibration |
| 1652 | 1654 | 1654 | 1651 | C = C stretching |
| 1723 | 1742 | – | – | C = O stretching vibration |
| 1377 | 1385 | 1385 | 1382 | $CH_3$ symmetric |
| 1246 | 1254 | 1254 | 1261 | C-O-C stretching |
| 1095 | 1102 | 1106 | 1091 | C-C asymmetric |
| | 672 | 672 | 672 | C-Cl stretching |

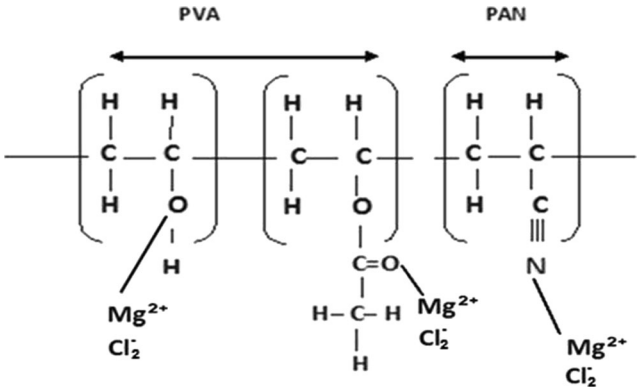


**Fig. 3** Possible interaction between blend polymer (PVA:PAN) and $MgCl_2$

the stretching vibration of nitrile (C≡N) in 92.5PVA:7.5PAN electrolyte at 2236 $cm^{-1}$ has disappeared which indicates the complexation of polymer. The peak absorbed at 672 $cm^{-1}$ in all the BPE's with different salt concentrations is ascribed to C-Cl stretching peak which confirm the $Cl^-$ ion in 92.5PVA:7.5PAN films with $MgCl_2$ [44, 45]. Thus the complexation of the host polymer with salt is proved by the appearance of new peak along with changes in existing peaks in the FTIR spectra.

## Differential scanning calorimetry (DSC)

In most of the polymeric materials, the crystalline and amorphous phases co-exist in variable amount. PVA blended with PAN membrane exhibits both amorphous and crystalline nature. For electrochemical applications, polymers with the $T_g$ below the operating temperature are more desirable [46]. Figure 4. represents the DSC curves for PVA:PAN/$MgCl_2$ blended samples in which their $T_g$ values are noted. Sivadevi et al. have reported $T_g$ value of the blend polymer

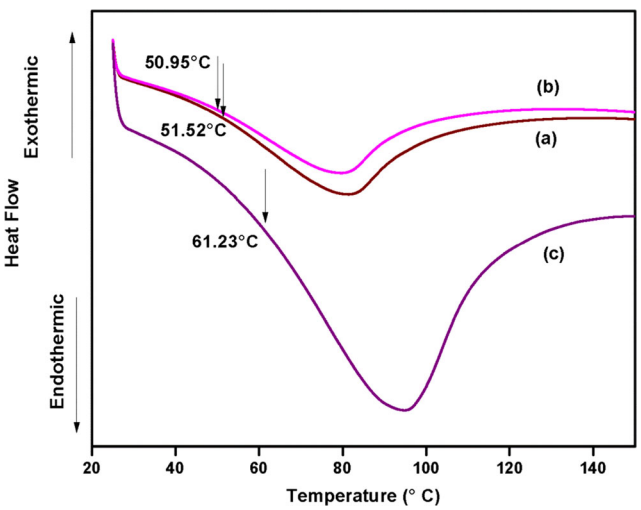


**Fig. 4** DSC thermogram in glass transition temperature (Tg) of (a) 92.5PVA:7.5PAN:0.4 m.m.% $MgCl_2$, (b) 92.5PVA:7.5PAN:0.5 m.m.% $MgCl_2$, and (c) 92.5PVA:7.5PAN:0.6 m.m.% $MgCl_2$

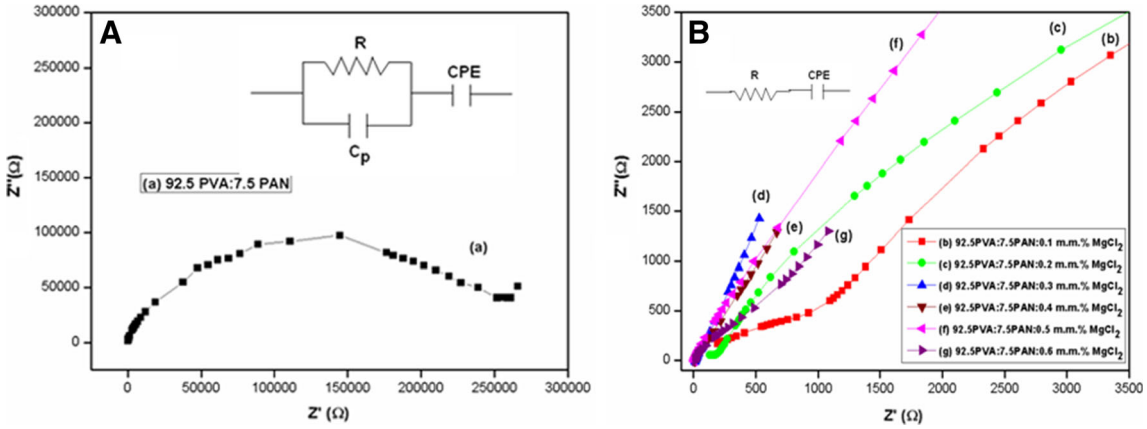


**Fig. 5** **A**- Nyquist plot for (a) 95.5PVA:7.5PAN. **B**- (b) 92.5PVA:7.5PAN:0.1 m.m.% $MgCl_2$, (c) 92.5PVA:7.5PAN:0.2 m.m.% $MgCl_2$, (d) 92.5PVA:7.5PAN:0.3 m.m.% $MgCl_2$, (e) 92.5PVA:7.5PAN:0.4 m.m.% $MgCl_2$, (f) 92.5PVA:7.5PAN:0.5 m.m.% $MgCl_2$, and (g) 92.5PVA:7.5PAN:0.6 m.m.% $MgCl_2$

92.5PVA:7.5PAN electrolyte as 136.4 °C [24]. It is observed from the curve that the $T_g$ values of the polymer-salt complexes decreases with the introduction of salt from 0.4 to 0.5 m.m. % $MgCl_2$. With increase in salt concentration, the $T_g$ value decreases which may be attributed to the plasticizing effect. 92.5PVA:7.5PAN:0.5 m.m. % $MgCl_2$ exhibits the minimum $T_g$ value of 50.95 °C. Similar result has been reported for the composition 92.5PVA:7.5PAN with 0.25 m.m.% $Mg(ClO_4)_2$ [47]. Further increase in the salt concentration causes an increase in the value of $T_g$ which may be due to the presence of undissociated salt in the polymer matrix [48].

## Impedance analysis

The ionic conductivity mainly depends on the conducting species and their mobility. Figure 5A, B shows Nyquist plots at room temperature (303 K) for 92.5PVA:7.5PAN and BPE complexed with $MgCl_2$ salt at various concentrations (0.1, 0.2, 0.3, 0.4, 0.5, 0.6 m.m.%). In the plots, presence of depressed semicircles shows non Debye nature of the polymer electrolytes [49]. Nyquist plots are fitted with semicircle and the respective bulk resistance ($R_b$) of each polymer electrolyte is determined from the point of intersection of higher end of semicircle with the real ($Z' = R_b$) axis [50]. From Fig. 5B, it is inferred that as the salt concentration increases, the polymer electrolytes have only inclined spike and the semicircle was not observed, which indicates that the BPE have resistive component only and the capacitive nature of electrolyte were vanished, which is due to the motion of charge carrier in the polymer electrolyte. The equivalent circuit was also shown in Fig. 5. Electrochemical impedance spectroscopy (EIS) parameters have been obtained from Nyquist plot by using EQ software program developed by Boukmap [51, 52], which were listed in Table 3. In Table 3, the resistance value of pure 92.5PVA:7.5PAN was obtained as $3.08 \times 10^5$ Ω, whereas for 0.1–0.5 m.m.% of $MgCl_2$ added with 92.5PVA:7.5PAN polymer electrolyte the value of resistance was decreased from $3.6 \times 10^3$ Ω to 5.7Ω and increases as 8.9 Ω for 0.6 m.m.% of $MgCl_2$. The constant phase element (CPE) which represents the effect of electrode and electrolyte interface value for pure 92.5PVA:7.5PAN was obtained as $4.15 \times 10^{-9}$ F. The $MgCl_2$ added with 92.5PVA:7.5PAN polymer electrolyte have CPE values in the range of 0.4 to 0.76 μF which were represented by low frequency spike. The highest conductivity polymer electrolyte 92.5PVA:7.5PAN:0.5 m.m.% $MgCl_2$ has $R_b = 5.7\Omega$ and CPE = $3.688 \times 10^{-5}\Omega$. The ionic conductivity ($\sigma$) of electrolyte films is estimated from following equation.

$$\sigma = {}^{tA}/_{R_b} \tag{3}$$

where $t$ and $A$ represent thickness and area of the polymer electrolyte, respectively.

The calculated ionic conductivity for different concentration of PVA:PAN:$MgCl_2$ BPE's at various temperatures is tabulated in Table 4. Table 4 illustrates that the ionic conductivity increases with increase in $MgCl_2$ and attains a maximum value of $1.01 \times 10^{-3}$ S $cm^{-1}$ at room temperature for 92.5PVA:7.5PAN:0.5 m.m.% $MgCl_2$. The increase in conductivity with the salt content is attributed to the increase in mobility of charge carriers in the system. This feature of increase in conductivity with the salt is an indication of the absence of

**Table 3** EIS parameter for all the prepared polymer electrolytes

| Polymer composition (m.m.%) | R(Ω) | CPE (F) | $n$ |
|---|---|---|---|
| Pure 92.5PVA:7.5PAN | $3.0813 \times 10^5$ | $4.1520 \times 10^{-9}$ | 0.7187 |
| 92.5PVA:7.5PAN:0.1 m.m.%. | $3.6165 \times 10^3$ | $5.7750 \times 10^{-6}$ | 0.4084 |
| 92.5PVA:7.5PAN:0.2 m.m.%. | $1.1750 \times 10^2$ | $1.0605 \times 10^{-5}$ | 0.4598 |
| 92.5PVA:7.5PAN:0.3 m.m.%. | $1.3172 \times 10$ | $8.9513 \times 10^{-5}$ | 0.7691 |
| 92.5PVA:7.5PAN:0.4 m.m.%. | 6.557 | $1.7276 \times 10^{-5}$ | 0.6934 |
| 92.5PVA:7.5PAN:0.5 m.m.%. | 5.7 | $3.688 \times 10^{-5}$ | 0.5356 |
| 92.5PVA:7.5PAN:0.6 m.m.%. | 8.9 | $7.2195 \times 10^{-6}$ | 0.6802 |

neutral pair formation due to salt agglomeration, which is often observed in polymer electrolyte systems at higher contents of salt. The continuous increase of conductivity with salt content is a sufficient proof for the maximum dissociation of the salt in the polymer matrix [53, 54]. It is observed that the further addition of $MgCl_2$ salts greater than 0.5 m.m.% decreases the conductivity due to the formation of more ion aggregates in the polymer network [55].

## Temperature-dependent conductivity

The temperature-dependent study has been used to analyze the possible mechanism of ionic conduction in BPE system. Figure 6 shows temperature dependence of ionic conductivity of BPEs in the temperature range 303 to 343 K. The highest conducting sample, 92.5PVA:7.5PAN:0.5 m.m.% $MgCl_2$, has an ionic conductivity of $1.1 \times 10^{-3}$ S $cm^{-1}$ at room temperature and $1.73 \times 10^{-3}$ S $cm^{-1}$ at 343 K. As the temperature increases, the polymer can expand easily and produce free volume. The increase in conductivity with temperature is attributed to increase the polymer chain mobility due to (i) increased free volume at higher temperature which facilitates the ions to hop between adjacent coordination sites and (ii) the equilibrium between dissociated and associated forms of $MgCl_2$ should favor the dissociated ions at higher temperatures [56]. The linear variation of ionic conductivity with inverse of absolute temperature follows Arrhenius relation

$$\sigma T = \sigma 0 \exp\left(^{-E_a}/_{KT}\right) \tag{4}$$

where, $\sigma_0$ is the pre-exponential factor, $E_a$ is the activation energy and $K$ is the Boltzmann constant. Activation energy ($E_a$) is the minimum energy required for the ion movement. $E_a$ values have been calculated for all prepared BPE's by the linear fitting of Arrhenius plots. Figure 7 relates the conductivity and activation energy values of all composition of 92.5PVA:7.5PAN:$MgCl_2$ polymer electrolyte, which were listed in Table 4. Table 4 indicates that the activation energy value of the polymer electrolyte decreases with increase in $MgCl_2$ concentration. The highest conducting sample posses the lowest activation energy.

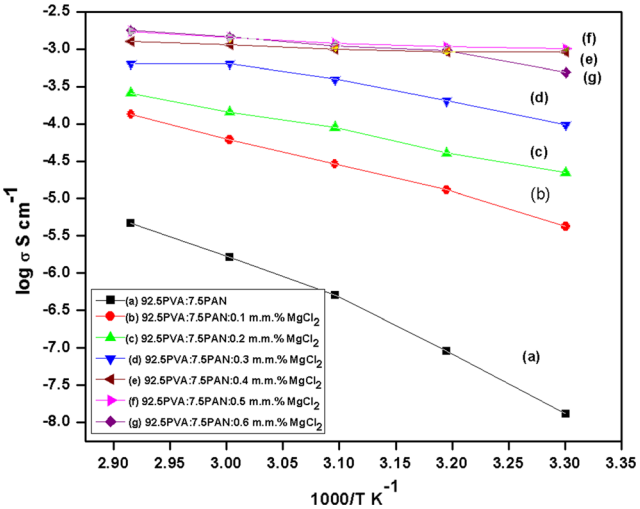


**Fig. 6** Temperature dependence ionic conductivity of 92.5PVA:7.5PAN polymer electrolyte with different $MgCl_2$ concentrations (a) pure (b) 0.1 m.m. %, (c) 0.2 m.m. %, (d) 0.3 m.m. %, (e) 0.4 m.m. %, (f) 0.5 m.m. %, and (g) 0.6 m.m. %

## Frequency-dependent conductivity

Figure 8 shows the frequency-dependent conductivity of 92.5PVA:7.5PAN polymer electrolytes with different contents of $MgCl_2$ at room temperature. From Fig. 8, it is evident that there is a low-frequency dispersion region which is due to electrode–electrolyte space charge polarization effects [57] and the frequency independent plateau region of the conductivity spectra signifies the migration of ions to neighboring sites. The low-frequency region leads to decrease in the number of mobile ions and conductivity due to the accumulation of charge at the electrode–electrolyte interface. The plateau region corresponds to DC conductivity ($\sigma_{dc}$) of the blend polymer electrolyte. From the ac conductivity spectra, it can be observed that the conductivity increases with the increase in the salt content. The increase in conductivity with the salt content is attributed to the increase in the number of charge carriers. The $\sigma_{dc}$ values for highest conductivity sample (92.5PVA:7.5PAN:0.5 m.m.%.$MgCl_2$) have been calculated by extrapolating the plateau region to log σ axis. The conductivity values obtained from the conduction spectra coincide with the bulk conductivity values obtained from Nyquist plot.

**Table 4** Ionic conductivity and activation energy values of 92.5PVA:7.5PAN: $MgCl_2$ BPEs for different temperatures

| | | | | | | | |
|---|---|---|---|---|---|---|---|
| Pure 92.5PVA:7.5PAN | $1.3 \times 10^{-8}$ | $1.56 \times 10^{-7}$ | $5.03 \times 10^{-7}$ | $3.28 \times 10^{-6}$ | $4.65 \times 10^{-6}$ | 1.33 | 0.94 |
| 92.5PVA:7.5PAN:0.1 m.m.%. | $4.22 \times 10^{-6}$ | $1.3 \times 10^{-5}$ | $2.9 \times 10^{-5}$ | $6.15 \times 10^{-5}$ | $1.35 \times 10^{-4}$ | 0.76 | 0.99 |
| 92.5PVA:7.5PAN:0.2 m.m.%. | $2.2 \times 10^{-5}$ | $4.05 \times 10^{-5}$ | $9 \times 10^{-5}$ | $1.43 \times 10^{-4}$ | $2.58 \times 10^{-4}$ | 0.55 | 0.99 |
| 92.5PVA:7.5PAN:0.3 m.m.%. | $4.37 \times 10^{-4}$ | $6.3 \times 10^{-4}$ | $8.2 \times 10^{-4}$ | $1.08 \times 10^{-3}$ | $1.32 \times 10^{-3}$ | 0.44 | 0.95 |
| 92.5PVA:7.5PAN:0.4 m.m.%. | $9.17 \times 10^{-4}$ | $9.19 \times 10^{-4}$ | $9.95 \times 10^{-4}$ | $1.14 \times 10^{-3}$ | $1.26 \times 10^{-3}$ | 0.11 | 0.95 |
| 92.5PVA:7.5PAN:0.5 m.m.%. | $1.01 \times 10^{-3}$ | $1.08 \times 10^{-3}$ | $1.20 \times 10^{-3}$ | $1.43 \times 10^{-3}$ | $1.73 \times 10^{-3}$ | 0.07 | 0.99 |
| 92.5PVA:7.5PAN:0.6 m.m.%. | $4.87 \times 10^{-4}$ | $9.57 \times 10^{-4}$ | $1.10 \times 10^{-3}$ | $1.45 \times 10^{-3}$ | $1.77 \times 10^{-3}$ | 0.27 | 0.94 |

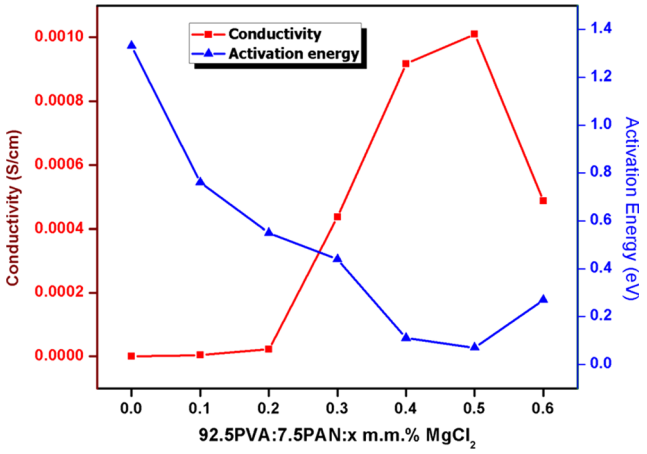


**Fig. 7** Concentration-dependent conductivity and activation energy

## Dielectric studies

The important insights into the ionic transport phenomenon were characterized using dielectric properties of 92.5PVA:7.5PAN(0.1, 0.2, 0.3, 0.4, 0.5 and 0.6 m.m%)$MgCl_2$ BPE's with frequency-dependent parameters [58]. Figures 9 and 10 show the variation of dielectric permitivity ε′ and dielectric loss ε″ versus frequency at room temperature 303 K. Figures 9 and 10 reveal that ε′ and ε″ increases at low frequencies which can be attributed to the formation of space charge region at the electrode–electrode interface which is familiarly known as $\omega^{n-1}$ variation or non-Debye type behavior where the space charge regions with respect to frequency is explained in terms of ion diffusion [59]. The dielectric constant (ε′) is high at low frequency due to the interfacial polarization and dielectric loss (ε″) becomes very large at lower frequencies due to free charge motion within the material [60]. At high frequency, due to the rapid periodic reversal of the applied electric field the mobile ion will not be able to orient them in the field direction

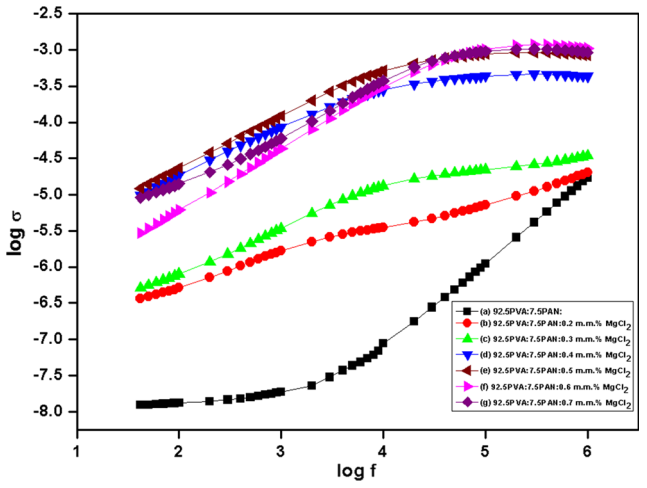


**Fig. 8** Frequency-dependent conductance spectra for 92.5PVA:7.5PAN polymer electrolyte with different $MgCl_2$ concentrations (a) pure (b) 0.1 m.m. %, (c) 0.2 m.m. %, (d) 0.3 m.m. %, (e) 0.4 m.m. %, (f) 0.5 m.m. %, and (g) 0.6 m.m. %

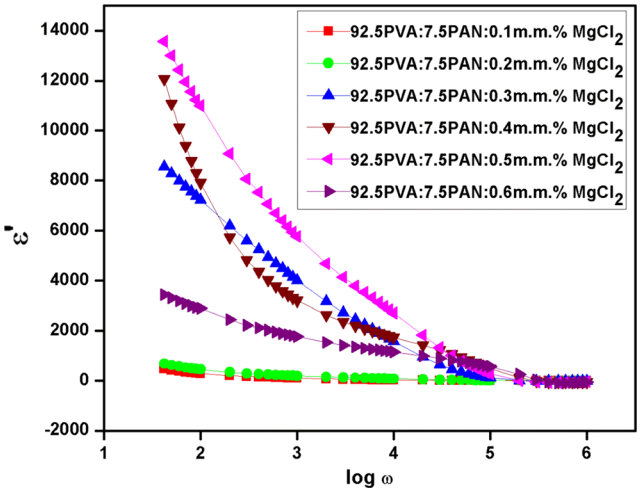


**Fig. 9** Plot of log ω vs. ε′ for BPEs with different concentrations of $MgCl_2$ at RT

which leads to saturate or decrease the dielectric constant [61]. The dielectric parameter values (ε′ and ε″) are found to be increased with salt-$MgCl_2$ content in polymer complexes. The higher value for both ε′ and ε″ have been observed for 92.5PVA:7.5PAN:0.5 m.m.%$MgCl_2$ at room temperature due to the localization of the charge carriers. This signifies that the degree of salt dissociation and redissociation of ion aggregates causes the increase in number of free ions which in turn increases the conductivity [62].

## Modulus spectra

The electric modulus spectra are a useful tool to investigate the ion transport process of ionic conductor. Figures 11 and 12 represent the frequency dependence of M′ (ω) and M″ (ω) at room temperature. At high frequency end both M′ and M″ are observed to increase. At low frequency, the value of both M′ and M″decreases due to the electrode polarization

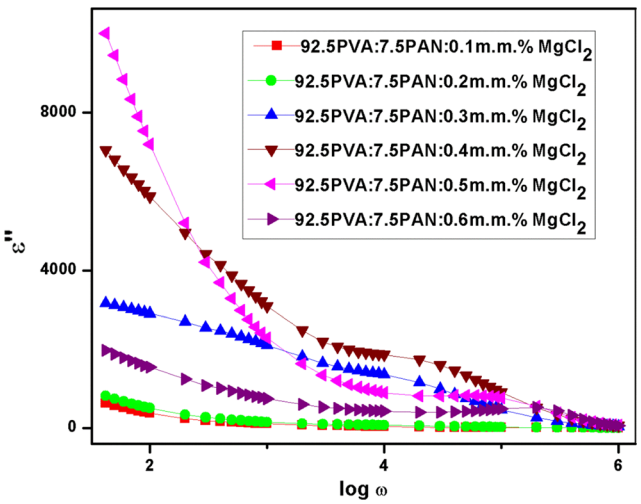


**Fig. 10** Plot of log ω vs. ε″ for BPEs with different concentrations of $MgCl_2$ at RT

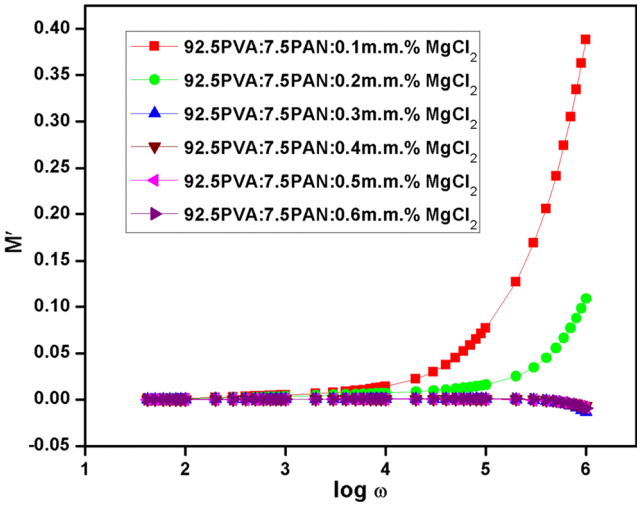


**Fig. 11** Variation of real part of modulus (M′) with frequency for BPEs with different concentrations of $Mg(ClO_4)_2$ at RT

phenomenon and makes a negligible contribution. Due to bulk effect for all the composition of 92.5PVA:7.5PAN:$MgCl_2$ BPE's the modulus value gradually increases with the increase of frequency. From the plot it is apparent that as the salt concentration increases the height of the plot decreases suggesting the fast relaxation of the ions. Long tails at low frequency sides are observed in the plot which indicates the large capacitance value associated with electrode polarization effects [57].

## Transport number measurement

To investigate the main conducting element in the BPE's transference number measurement (TNM) has been carried out using the DC polarization method as described in Section 2. Figure 13b (i) shows the variation of polarizing current through a typical cell: SS|92.5PVA:7.5PAN:0.5 m.m.% $MgCl_2$|SS as a function of time on applying a voltage of 1 V. Due to the

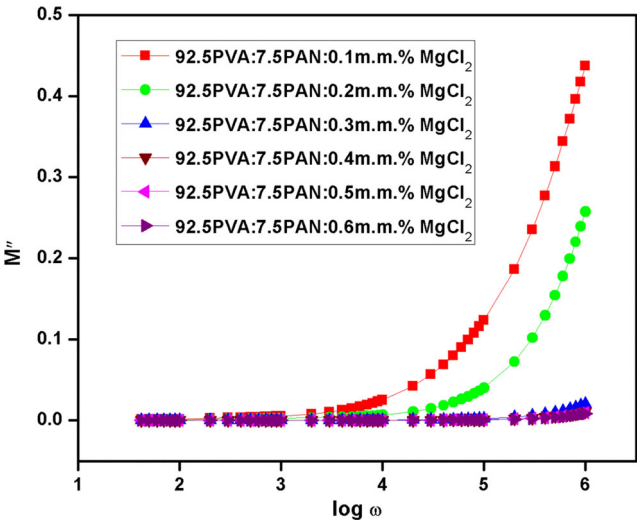


**Fig. 12** Variation of imaginary part of modulus (M″) with frequency for BPE's with different concentrations of $Mg(ClO_4)_2$ at RT

depletion of ionic species in the electrolyte, the initial total current ($t_i$) has been found to decrease with time and become constant in the fully depleted situation. At the steady state, the cell is polarized and because of electron migration the current flows across the electrolyte and interfaces. The value of $t_{ion}$ is determined using Eq. (1) and found to be > 0.98 for all the BPE films. This shows that the overall conductivity of the BPE's is predominantly ionic. The present system consists of both cations ($Mg^{2+}$) and anions ($Cl^{2-}$) which are the mobile charge carriers, among which the transport no of $Mg^{2+}$ ions are calculated to determine the performance of the BPE. The transport number ($t_+$) of $Mg^{2+}$ ions in the BPE films are obtained from a combination of AC and DC techniques, as proposed by Evans et al. [29]. In this technique, the transport number, $t_+$ of $Mg^{2+}$ ions for the highest conducting film was evaluated using the symmetrical cell Mg/BPE/Mg. The cell was polarized by applying a small D.C. voltage of 1.5 V and the initial ($I_0$) and the final ($I_s$) current values were noted from the current-time plot as shown as in Fig. 13b (ii). Using impedance measurements, the cell resistances before and after polarization $R_o$ and $R_s$ respectively were obtained. The impedance plots are shown in Fig. 13a, the intercept at the high-frequency region corresponds to the impedance of the bulk electrolyte, $R_b$. The fitting of the impedance plots was carried out by using EQ software [51, 52]. The diameter of the semicircle at the low-frequency region has formed from the total impedance of the cell, ($R_s = R_b + R_i$), where $R_i$ is the resistance of the passivation layer [63] indicating that the passivation layer is continued to grow during polarization. Choe et al. and Abraham et al. have been reported the similar behavior for polymer electrolytes based on polyacrylonitrile and poly(vinylidene fluoride)-hexafluoropropene, respectively [63, 64]. The values of $Mg^{2+}$ transport number were calculated using the formula,

$$t+ = \frac{I_s\,(\Delta V - R_0 I_0)}{I_0(\Delta V - R_s I_s)} \tag{5}$$

where $I_o$ and $I_s$ are the initial and the final current, respectively. $R_o$ and $R_s$ are the cell resistance before and after polarization, respectively. The values of $Mg^{2+}$ ion transport number were calculated to be 0.38 for the highest conducting film of the 92.5PVA:7.5PAN:0.5 m.m.% $MgCl_2$ system. This value suggests a significant contribution of $Mg^{2+}$ to the total ionic conduction of the BPE films. Kumar et al. have reported the values of the transport number for the $Mg^{2+}$ ion in his work as 0.33 for PMMA-based GPE system using 0.5 g of $Mg(CF_3SO_3)_2$ salt [65].

## Linear sweep voltammetry (LSV)

The working cell potential of an electrolyte can be investigated using electrochemical stability. The electrochemical stability of a polymer electrolyte has been examined by

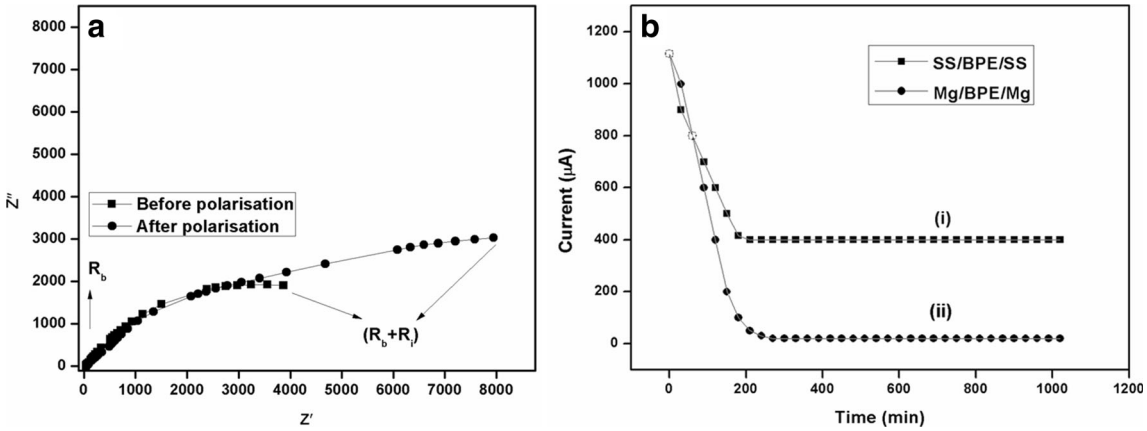


**Fig. 13** **a** A.C. complex impedance plot before and after polarization of a typical symmetric Mg/92.5PVA:7.5PAN:0.5 m.m.% $MgCl_2$/Mg cell. **b** D.C. polarizaton curve of (i) SS/92.5PVA:7.5PAN:0.5 m.m.% $MgCl_2$ /SS cell and (ii) Mg/92.5PVA:7.5PAN:0.5 m.m.% $MgCl_2$ /Mg cell at room temperature

linear sweep voltammetry. The optimized conducting BPE sample has been placed between SS and Mg electrode as SS|92.5PVA:7.5PAN:0.5 m.m.%$MgCl_2$ |Mg and scanned curve at a rate of 5 $mVs^{-1}$ has been recorded as shown in Fig. 14. Due to the decomposition of the electrolyte at the blocking electrode, sudden rise in the current is observed from the plot which in turn shows the electrochemical stability window of 3.66 V. The result shows that the electrolyte is convenient for its application in magnesium ion batteries [66]. Osman et al. have obtained the stability window of 3.5 V for the electrolyte system SS/PVDF-HFP:20 wt%$(Mg(CF_3SO_3))_2$/Mg [67].

## Performance of Mg cell

The applicability of the blend polymer electrolyte to rechargeable magnesium battery system has been examined by fabricating a prototype cell. For the cathode material of the cell an amount of $MnO_2$ (1 g) and graphite (0.1 g) were mixed together and pressed with 5 ton pressure to form a pellet. To introduce the electronic conductivity graphite was added. For cell anode, magnesium metal in pellet form was chosen. The highest conducting BPE(92.5PVA:7.5PAN:0.5 m.m.% $MgCl_2$) was sandwiched between anode and cathode in battery holder. Figure 15. represents the schematic diagram of fabricated cell.

The open circuit potential (OCP) of the cell as a function of time at room temperature is shown in Fig. 16A. The initial voltage of 2.17 V which has been found to be slightly reduced to ~ 1.85 V in the first 200 h of assembly. Similar OCP of 2.3 V was reported by Kumar et al., for magnesium gel polymer electrolyte [68]. The stabilized potential of 1.85 V has been observed for a period of 1 month. Due to the cell formation reaction at the electrodes the intermediate drop in the voltage of the cell after fabrication has been observed. The chemical reaction that probably take place in the cell are [47]:

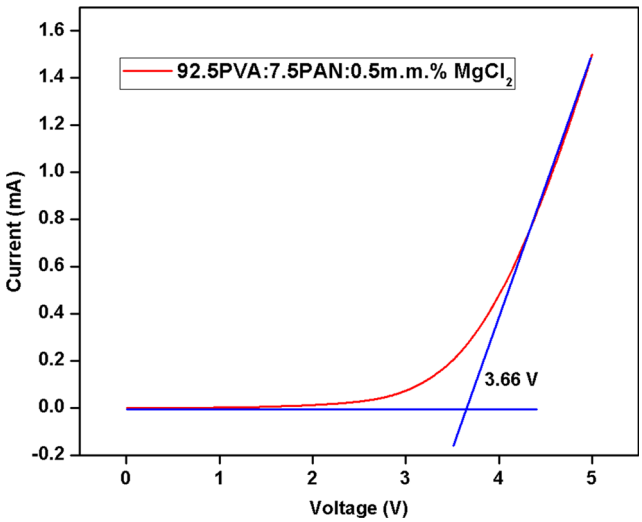


**Fig. 14** Linear sweep voltammetry of SS/92.5PVA:7.5PAN:0.5 m.m.% $MgCl_2$/Mg cell recorded at a scan rate of 5 mV $s^{-1}$ at room temperature

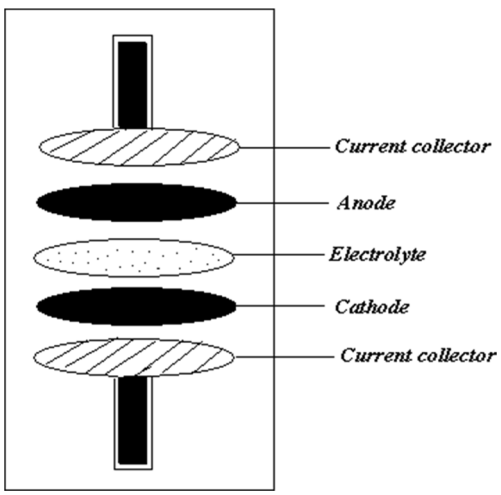


**Fig. 15** Schematic diagram of battery configuration

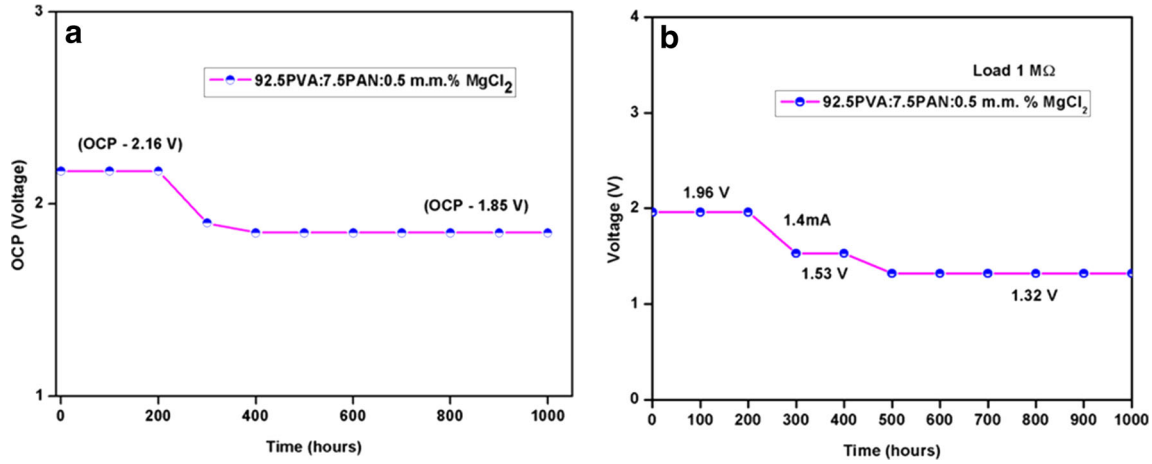


**Fig. 16** **a** Open circuit potential as a function of time for 92.5PVA:7.5PAN:0.5 m.m.% $MgCl_2$ BPE. **b** Discharge curves of cell using 1 MΩ for 92.5PVA:7.5PAN:0.5 m.m.% $MgCl_2$ BPE

At the anode:

$$Mg + 2(OH^-) \rightarrow Mg(OH)_2 + 2e \quad (6)$$

At the cathode:

$$2MnO_2 + H_2O + 2e \rightarrow Mn_2O_3 + 2OH^- \quad (7)$$

Overall reaction

$$Mg + 2MnO_2 + H_2O \rightarrow Mn_2O_3 + Mg(OH)_2 \quad (8)$$

In the host polymer PVA:PAN, the molecular structure of PVA contains hydroxyl group which may be source of hydroxide ion in Mg-MnO2 battery. It is also known that PVA will have occluded moisture/$H_2O$ (occluded water is a type of non-essential water which is retained due to physical forces in microscopic pores spaced irregularly throughout the solid polymer PVA) which may be the source of hydroxyl ion. The theoretical oxidation potential of Mg is known to be − 2.37 V, and the reduction potential of $MnO_2$ is known to be 1.23 V [69]. The overall reaction should provide the cell with $E_o$ = 3.6 V. However, the cell Mg/92.5PVA:7.5PAN:0.25 m.m.%$MgCl_2$/$MnO_2$ provides a voltage of $E$ = 2.17 V. The difference between the theoretical and the experimental open circuit potentials may be due to the possible reduction of the $MnO_2$ which results in a reduced cummulative voltage being provided by the electrode's reaction.

Figure 16B shows the discharge characteristics of the cell at room temperature by connecting it to an external load of 1 MΩ. The initial decrease in potential of this cell may be due to the polarization effect at the electrode electrolyte interface [70]. The cell potential discharged at a constant load of 1MΩ remains constant at 1.96 V which reduces to 1.53 V after dropping a short circuit current of 1.4 mA for 24 h and then it is decreased to 1.32 V and retained it for 1 month. The region in which the cell voltage remains constant is called as plateau region. The cell parameters are given in Table 5.

## Conclusion

The new BPEs based on 92.5PVA:7.5PAN:x$MgCl_2$ with various concentrations ($x$ = 0.1–0.6 m.m.%) have been prepared by solution casting technique and characterized. On the basis of various structural, thermal, electrical, and electrochemical studies, the following conclusions have been drawn:

(i) The polymer blend electrolyte film is flexible and free-standing with good mechanical strength.
(ii) The composite nature of the blend polymer electrolyte films due to dispersion of $MgCl_2$ salt is confirmed through XRD results.
(iii) The existence of free chloride ion–polymer interaction has also been detected from the FTIR studies.
(iv) The film 92.5PVA:7.5PAN:0.5 m.m.% $MgCl_2$ offers high ionic conductivity $1.1 \times 10^{-3}$ S $cm^{-1}$ at room temperature. The temperature-dependent ionic conductivity of this highest conducting BPE obeys the Arrhenius relationship with low activation energy. The electrode polarization, polymer segmental motion, conductivity relaxation and the distribution of the relaxation times in the BPE's have been confirmed by measuring dielectric spectra and electric modulus.

**Table 5** Cell parameters

| Cell parameters | Measured values of discharge through 1MΩ |
|---|---|
| Cell area ($cm^2$) | 1.23 |
| Cell weight (g) | 1.1 |
| Effective cell diameter (cm) | 1.2 |
| Cell thickness (cm) | 0.55 |
| Open circuit voltage (V) | 2.17 |
| Current drawn (mA) | 1.4 |
| Discharge time for plateau region (h) | 500 |

(v) Thermal analysis indicates that the glass transition temperature is low for the 92.5PVA:7.5PAN:0.5 m.m.% $MgCl_2$ polymer electrolyte .

(vi) The transport number indicates that the dominant conducting species are found to be ions rather than electrons.

(vii) The electrochemical stability window, estimated from LSV is found to be 3.6 V, which is sufficient for electrochemical applications.

(viii) Thus, the optimized BPE 92.5PVA:7.5PAN:0.5 m.m.% $MgCl_2$ with high ionic conductivity has been applied for primary magnesium battery application, in which their main parameters and out-put potential were reported.

## References


1. Tarascon JM, Armand M (2001) Issues and challenges facing rechargeable lithium batteries. Nature 414:359–367
2. Zhang J, Zhao J, Yue L, Wang Q, Chai J, Liu Z et al (2015) Safety-reinforced poly (propylene carbonate)-based all-solid-state polymer electrolyte for ambient-temperature solid polymer lithium batteries. Adv Energy Mater 5(24)
3. Kaplan ML, Rietman EA, Cava RJ, Holt LK, Chandross EA (1987) Crown ether enhancement of ionic conductivity in a polymer-salt system. Solid State Ionics 25(1):37–40
4. Roux C, Gorecki W, Sanchez JY, Belorizky E (1998) Various aspects of dynamical properties of high and low molecular weight PPO-LITFSI polymer electrolytes obtained by NMR techniques. Electrochim Acta 43(10):1575–1579
5. Shukla, P.K. and Agrawal, S.L. (1998) Proceedings of the 6th Asian Conference on Solid State Ionics, New Delhi India
6. Subban RH, Arof AK (2003) Experimental investigations on PVC-LiCF3SO3-SiO 2 composite polymer electrolytes. J New Mater Electrochem Syst 6(3):197–203
7. Mohamed NS, Arof AK (2004) Investigation of electrical and electrochemical properties of PVDF-based polymer electrolytes. J Power Sources 132(1):229–234
8. Stephan AM, Thirunakaran R, Renganathan NG, Sundaram V, Pitchumani S, Muniyandi N, Gangadharan R, Ramamoorthy P (1999) A study on polymer blend electrolyte based on PVC/PMMA with lithium salt. J Power Sources 81:752–758
9. Morales E, Acosta JL (1997) Thermal and electrical characterization of plasticized polymer electrolytes based on polyethers and polyphosphazene blends. Solid State Ionics 96(1–2):99–106
10. Ulaganathan M, Mathew CM, Rajendran S (2013) Highly porous lithium-ion conducting solvent-free poly (vinylidene fluoride-co-hexafluoropropylene)/poly (ethyl methacrylate) based polymer blend electrolytes for Li battery applications. Electrochim Acta 93:230–235
11. Rajendran S, Sivakumar M, Subadevi R (2004) Investigations on the effect of various plasticizers in PVA–PMMA solid polymer blend electrolytes. Mater Lett 58(5):641–649
12. Reddy CVS, Sharma AK, Rao VN (2002) Effect of plasticizer on electrical conductivity and cell parameters of PVP+ PVA+ KClO 3 blend polymer electrolyte system. J Power Sources 111(2):357–360
13. Subramania A, Kalyana Sundaram NT, Vijaya Kumar G, Vasudevan T (2006) New polymer electrolyte based on (PVA–PAN) blend for li-ion battery applications. Ionics 12:175–178
14. Rudhziah S, Mohamed NS (2009) Characterization of proton conducting PVDF-HFP/PEMA blend based solid electrolytes. Solid State Sci Technol 17(1):73–80
15. Lee JH, Lee HB, Andrade JD (1995) Blood compatibility of polyethylene oxide surfaces. Prog Polym Sci 20(6):1043–1079
16. Robeson LM, Hale WF, Merriam CN (1981) Miscibility of the poly (hydroxy ether) of bisphenol A with water-soluble polyethers. Macromolecules 14(6):1644–1650
17. Song JY, Wang YY, Wan CC (1999) Review of gel-type polymer electrolytes for lithium-ion batteries. J Power Sources 77(2):183–197
18. Sivadevi S, Selvasekarapandian S, Karthikeyan S, Vijaya N, Kingslin Mary Genova F, Sanjeeviraja C (2013) Structural and AC impedance analysis of blend polymer electrolyte based on PVA and PAN. Int J Sci Res 2(10)
19. Vignarooban K, Kushagra R, Elango A, Badami P, Mellander BE, Xu X, Tucker TN, C., & Kannan, A. M. (2016) Current trends and future challenges of electrolytes for sodium-ion batteries. Int J Hydrog Energy 41(4):2829–2846
20. Ramaswamy M, Malayandi T, Subramanian S, Srinivasalu J, Rangaswamy M (2017) Magnesium ion conducting polyvinyl alcohol–polyvinyl pyrrolidone-based blend polymer electrolyte. Ionics 23(7):1771–1781
21. Sundar M, Selladurai S (2006) Effect of fillers on magnesium–poly (ethylene oxide) solid polymer electrolyte. Ionics 12(4–5):281–286
22. Pandey GP, Hashmi SA (2009) Experimental investigations of an ionic-liquid-based, magnesium ion conducting, polymer gel electrolyte. J Power Sources 187(2):627–634
23. Sivadevi S, Selvasekarapandian S, Karthikeyan S, Vijaya N, Kingslin F, Genova, Sanjeeviraja C, Nithya H & Kawamura IJ (2013) Proton-conducting polymer electrolyte based on PVA-PAN blend polymer doped with NH4NO3. Int J Electroact Mater (1), 64–70
24. Sivadevi S, Selvasekarapandian S, Karthikeyan S, Sanjeeviraja C, Nithya H, Iwai Y, Kawamura J (2014) Proton-conducting polymer electrolyte based on PVA-PAN blend doped with ammonium thiocyanate. Ionics (21):1017-1029
25. Kingslin Mary Genova F, Selvasekarapandian S, Karthikeyan S, Vijaya N, Pradeepa R, Sivadevi S (2015) Study on blend polymer (PVA_PAN) doped with lithium bromide. Polymer Sci 57:851–862
26. Francis KMG, Subramanian S, Shunmugavel K, Naranappa V, Pandian SSM, Nadar SC (2016) Lithium ion-conducting blend polymer electrolyte based on PVA–PAN doped with lithium nitrate. Polym-Plast Technol Eng 55(1):25–35
27. Mohamoud MA, Hillman AR (2007) The effect of anion identity on the viscoelastic properties of polyaniline films during electrochemical film deposition and redox cycling. Electrochim Acta 53(3):1206–1216
28. Hashmi SA, Chandra S (1995) Experimental investigations on a sodium-ion-conducting polymer electrolyte based on poly (ethylene oxide) complexed with NaPF6. Mater Sci Eng B 34(1):18–26
29. Evans J, Vincent CA, Bruce PG (1987) Electrochemical measurement of transference numbers in polymer electrolytes. Polymer 28(13):2324–2328
30. Agrawal RC, Hashmi SA, Pandey GP (2007) Electrochemical cell performance studies on all-solid-state battery using nano-composite polymer electrolyte membrane. Ionics 13(5):295–298
31. Sridevi D, Rajendran KV (2009) Synthesis and optical characteristics of ZnO nanocrystals. Bull Mater Sci 32(2)
32. Hodge RM, Edward GH, Simon GP (1996) Water absorption and states of water in semicrystalline poly (vinyl alcohol) films. Polymer 37(8):1371–1376
33. Baskaran R, Selvasekarapandian S, Kuwata N, Kawamura J, Hattori T (2006) Conductivity and thermal studies of blend polymer electrolytes based on PVAc–PMMA. Solid State Ionics 177(26):2679–2682

34. Novák P, Imhof R, Haas O (1999) Magnesium insertion electrodes for rechargeable nonaqueous batteries—a competitive alternative to lithium? Electrochimica Acta 45(1):351–367
35. Abdelaziz M, Abdelrazek EM (2007) Effect of dopant mixture on structural, optical and electron spin resonance properties of polyvinyl alcohol. Physica B: Condensed Matter 390(1):1–9
36. Wu KH, Wang YR, Hwu WH (2003) FTIR and TGA studies of poly (4-vinylpyridine-co-divinylbenzene)–Cu (II) complex. Polym Degrad Stab 79(2):195–200
37. Laot CM, Marand E, Oyama HT (1999) Spectroscopic characterization of molecular interdiffusion at a poly (vinyl pyrrolidone)/vinyl ester interface. Polymer 40(5):1095–1108
38. Li X, Goh SH, Lai YH, Wee ATS (2000) Miscibility of carboxyl-containing polysiloxane/poly (vinylpyridine) blends. Polymer 41(17):6563–6571
39. Stupp SI, Carr SH (1977) Chemical origin of thermally stimulated discharge currents in polyacrylonitrile. J Polym Sci B Polym Phys 15(3):485–499
40. Coleman MM, Petcavich RJ (1978) Fourier transform infrared studies on the thermal degradation of polyacrylonitrile. J Polym Sci B Polym Phys 16(5):821–832
41. Pandey GP, Agrawal RC, Hashmi SA (2011) Magnesium ion-conducting gel polymer electrolytes dispersed with fumed silica for rechargeable magnesium battery application. J Solid State Electrochem 15(10):2253–2264
42. Chen HW, Xu H, Huang CF, Chang FC (2004) Novel polymer electrolyte composed of poly (ethylene oxide), lithium triflate, and benzimidazole. J Appl Polym Sci 91(2):719–725
43. Su'ait MS, Ahmad A, Badri KH, Mohamed NS, Rahman MYA, Ricardo CA, Scardi P (2014) The potential of polyurethane bio-based solid polymer electrolyte for photoelectrochemical cell application. Int J Hydrogen Energy 39(6):3005–3017
44. Koenig J L 1999 Spectroscopy of polymers (Amsterdam:Elsevier) 2nd ed
45. Pavia D L, Lampman G M and Kriz G S (2001) Introduction to spectroscopy (Fort Worth: Harcourt College Publishers) 3rd ed
46. MacCallum JR, & Vincent CA (Eds.). (1989) Polymer electrolyte reviews (Vol. 2). Springer Science & Business Media
47. Manjuladevi R, Thamilselvan M, Selvasekarapandian S, Mangalam R, Premalatha M, Monisha S (2017) Mg-ion conducting blend polymer electrolyte based on poly (vinyl alcohol)-poly (acrylonitrile) with magnesium perchlorate. Solid State Ionics 308:90–100
48. Flora XH, Ulaganathan M, Rajendran S (2012) Influence of lithium salt concentration on PAN-PMMA blend polymer electrolytes. Int J Electrochem Sci 7:7451–7462
49. Lanfredi S, Saia PS, Lebullenger R, Hernandes AC (2002) Electric conductivity and relaxation in fluoride, fluorophosphate and phosphate glasses: analysis by impedance spectroscopy. Solid State Ionics 146(3):329–339
50. Mishra R, Baskaran N, Ramakrishnan PA, Rao KJ (1998) Lithium ion conduction in extreme polymer in salt regime. Solid State Ionics 112(3):261–273
51. Boukamp BA (1986) A nonlinear least squares fit procedure for analysis of immittance data of electrochemical systems. Solid State Ionics 20(1):31–44
52. Boukamp BA (1986) A package for impedance/admittance data analysis. Solid State Ionics 18:136–140
53. Aziz SB (2013) Li+ ion conduction mechanism in poly (ε-caprolactone)-based polymer electrolyte. Iran Polym J 22(12): 877–883
54. Lim YJ, An YH, Jo NJ (2012) Polystyrene-Al 2 O 3 composite solid polymer electrolyte for lithium secondary battery. Nanoscale Res Lett 7(1):19
55. Ramya CS, Selvasekarapandian S, Savitha T, Hirankumar G, Baskaran R, Bhuvaneswari MS, Angelo PC (2006) Conductivity and thermal behavior of proton conducting polymer electrolyte based on poly (N-vinyl pyrrolidone). Eur Polym J 42(10):2672–2677
56. Druger SD, Ratner MA, Nitzan A (1986) Applications of dynamic bond percolation theory to the dielectric response of polymer electrolytes. Solid State Ionics 18:106–111
57. Ramesh S, Arof AK (2001) Ionic conductivity studies of plasticized poly (vinyl chloride) polymer electrolytes. Mater Sci Eng B 85(1): 11–15
58. J.R. Mac Callum, C.A. Vincent (1989). Low frequency dielectric properties of polyether electrolytes. Elsevier Appl. Sci. 43–60
59. Macdonald JR (ed) (1987) Impedance spectroscopy. Wiley
60. Kyritsis A, Pissis P, Grammatikakis J (1995) Dielectric relaxation spectroscopy in poly (hydroxyethyl acrylates)/water hydrogels. J Polym Sci B Polym Phys 33(12):1737–1750
61. Adachi K, Urakawa O (2002) Dielectric study of concentration fluctuations in concentrated polymer solutions. J Non-Cryst Solids 307:667–670
62. Shastry MCR, Rao KJ (1991) Ac conductivity and dielectric relaxation studies in AgI-based fast ion conducting glasses. Solid State Ionics 44(3–4):187–198
63. Kumar Y, Hashmi SA, Pandey GP (2011) Ionic liquid mediated magnesium ion conduction in poly (ethylene oxide) based polymer electrolyte. Electrochim Acta 56(11):3864–3873
64. Abraham KM, Jiang Z, Carroll B (1997) Highly conductive PEO-like polymer electrolytes. Chem Mater 9(9):1978–1988
65. Kumar GG, Munichandraiah N (2002) Poly (methylmethacrylate)—magnesium triflate gel polymer electrolyte for solid state magnesium battery application. Electrochim Acta 47(7):1013–1022
66. Pandey GP, Agrawal RC, Hashmi SA (2011) Performance studies on composite gel polymer electrolytes for rechargeable magnesium battery application. J Phys Chem Solids 72(12):1408–1413
67. Rosdi A, Zainol NH, & Osman Z (2016) Ionic transport and electrochemical stability of PVDF-HFP based gel polymer electrolytes. In AIP Conference Proceedings (Vol. 1711, No. 1, p. 050003). AIP Publishing
68. Kumar GG, Munichandraiah N (2000) Solid-state Mg/MnO 2 cell employing a gel polymer electrolyte of magnesium triflate. J Power Sources 91(2):157–160
69. Kadir MFZ, Majid SR, Arof AK (2010) Plasticized-chitosan-PVA blend polymer electrolyte based proton battery. Electrochimca Acta 55:1475–1482
70. Reddy CVS, Sharma AK, Rao VN (2003) Conductivity and discharge characteristics of polyblend (PVP+ PVA+ KIO 3) electrolyte. J Power Sources 114(2):338–345